International Journal of Remote Sensing
Vol. 29, No. 21, 10 November 2008, 6281–6296

Taylor & Francis
Taylor & Francis Group

Automatic detection and tracking of oil spills in SAR imagery with level set segmentation

K. KARANTZALOS* and D. ARGIALAS

Remote Sensing Laboratory, School of Rural and Surveying Engineering, National Technical University of Athens, Iroon Polytechniou 9, 15780, Zografou Campus, Athens, Greece

(*Received 3 May 2007; in final form 2 May 2007*)

Automatic detection and monitoring of oil spills and illegal oil discharges is of fundamental importance in ensuring compliance with marine legislation and protection of the coastal environments, which are under considerable threat from intentional or accidental oil spills, uncontrolled sewage and wastewater discharged. In this paper, the level set based image segmentation was evaluated for the real-time detection and tracking of oil spills from SAR imagery. The processing scheme developed consists of a pre-processing step, in which an advanced image simplification takes place, followed by a geometric level set segmentation for the detection of possible oil spills. Finally, a classification was performed for the separation of look-alikes, leading to oil spill extraction. Experimental results demonstrate that the level set segmentation is a robust tool for the detection of possible oil spills, copes well with abrupt shape deformations and splits and outperforms earlier efforts that were based on different types of thresholds or edge detection techniques. The developed algorithm's efficiency for real-time oil spill detection and monitoring was also tested.

1. Introduction

Oil pollution from shipping constitutes one of the environmental concerns on which much international cooperation and law making has taken place. Already, there are numerous international treaties and regional conventions that have been adopted to deal with accidental and intentional oil discharges from vessels. In particular, in Europe, which is the world's largest market in crude oil imports, representing about one third of the world's total, 90% of oil and refined products are transported to and from the continent by sea; unfortunately, some of this oil makes its final way into the sea. Of the oil released by ships, 75% is estimated to have come from operational discharges and only 25% from accidental spills (Indregard *et al.* 2004). Furthermore, while past statistical assessments identified tankers as the main marine polluters with crude oil (by releasing oily mixture in ballast water or in cargo tank washings) recent assessments also give emphasis to all types of ships that may release oily mixtures in fuel oil sludge, in bilges and in engine room effluent discharges (al-Khudhairy 2002).

Towards the compliance with marine legislation and the efficient surveillance and protection of coastal environments, automatic detection and tracking of oil spills and illegal oil discharges is of fundamental importance. The construction of a cost-effective remote sensing processing system has been the subject of research and

*Corresponding author. Email: karank@central.ntua.gr

International Journal of Remote Sensing
ISSN 0143-1161 print/ISSN 1366-5901 online © 2008 Taylor & Francis
http://www.tandf.co.uk/journals
DOI: 10.1080/01431160802175488

development for approximately two decades (Bern *et al.* 1992, Skøelv and Wahl 1993, Wahl *et al.* 1994, Solberg *et al.* 2003), looking forwards, nowadays, to the construction of a fully automatic system that will identify objects with a high probability of being oil spills and will activate an alarm for further manual inspection and possible verification of the incident by a surveillance aircraft (Indregard *et al.* 2004, Brekke and Solberg 2005, EMSA 2007). Among the available remote sensing satellite data, spaceborne synthetic aperture radar (SAR) imagery is the most efficient and superior satellite sensor for oil spill detection, although it does not have capabilities for oil spill thickness estimation and oil type recognition (Fingas and Brown 1997). RADARSAT-1 and ENVISAT are the two main daily providers of satellite SAR images for oil spill monitoring. Access to an increased amount of SAR images means an increased image processing time.

Algorithms for automatic detection are, thus, of great benefit in helping to screen data and prioritise alarms for further inspection and verification. The major difficulty for such an effective detection is the resemblance between the SAR intensity signatures of oil spills and other features called look-alikes, which all appear with low intensity values in radar images. Detection algorithms that have been proposed in the literature suffer from false alarms, and slicks classified as oil spills may be confused with look-alikes (Brekke and Solberg 2005). Not all the dark areas on the SAR images of the sea surface are real oil spills and, in particular, a set of one hundred images may contain thousands of look-alikes and only hundreds of oil spills (Solberg *et al.* 2007). Oil spills appear with dark intensities, as oil dampens the short surface waves, and look-alikes appear with similar intensities due to certain atmospheric and oceanic phenomena such as natural films and slicks, algae, grease ice, areas with low wind speed and others (Espedal and Johannessen 2000).

The discrimination between oil spills and look-alikes is usually carried out with the use of a classification procedure based on the different values of certain characteristics that have been observed and reported both for oil slicks and for look-alikes. Such characteristics include the geometry, the shape, the texture and other contextual information describing the slick in relation to its surroundings (Brekke and Solberg 2005). Different classifiers have been proposed in the literature, such as a statistical classifier with rule-based modification of prior probabilities (Solberg *et al.* 1999, Solberg *et al.* 2007), the Mahalanobis classifier (Fiscella *et al.* 2000), a neural-network classifier (Del Frate *et al.* 2000), a fuzzy network (Keramitsoglou *et al.* 2006), etc. More details of the various methods can be found in the review paper by Brekke and Solberg (2005). Since, almost all methods are classifying segments and not pixels, the initial step of segmentation, which leads to the extraction of possible oil spill areas, is of major importance. If, during the segmentation step, a slick is not extracted, it will not be processed during the classification and alarm activation is impossible. In addition, a segmentation that leads to the extraction of many look-alikes can make the classification more difficult (Solberg *et al.* 2007) and thus the use of an advanced segmentation method is of major importance.

Segmentation methods that have been proposed in the literature for the detection of possible oil spills include: (i) fuzzy clustering (Barni *et al.* 1995), (ii) threshold-based techniques such as hysteresis thresholding (Kanaa *et al.* 2003) and an adaptive thresholding in one or more resolutions (Solberg *et al.* 1999, 2007), (iii) edge detection (Change *et al.* 1996, Chen *et al.* 1997, Migliaccio *et al.* 2005), wavelets

(Liu *et al.* 1997, Wu and Liu 2003) and mathematical morphology (Gasull *et al.* 2002) and (iv) QinetiQ's algorithm that combines a clustering and a Hough transform to identify linear targets (Indregard *et al.* 2004). Note that the above methods (ii, iii and iv) include a thresholding step during their computation, which leads to limitations such as over-segmentation or pure description of image regions.

In this paper, the use of a more sophisticated technique for image segmentation, which is based on the geometric level set method and which acts globally in the image, in contrast to pixel-based threshold methods is presented. The developed SAR image processing scheme consists of a pre-processing step, in which an image simplification takes place, followed by a geometric level set segmentation for the detection of possible oil spills. Finally, a classification, aiming at the separation of look-alikes, leading to oil spill extraction is performed.

2. Level set segmentation

Since the early 1990s, both in remote sensing (Argialas and Harlow 1990, Jensen 2000, Lillesand *et al.* 2003) and computer vision (Perona and Malik 1990, Paragios *et al.* 2005) communities, the fact that efficient object detection from images demands advanced image processing techniques has been addressed. Standard segmentation methods, such as using thresholds, yield limited results and, particularly for SAR imagery, a constant threshold value for the whole image cannot be recommended as the mean level of the background varies, even in a homogeneous sea, due to the image acquisition system (Gasull *et al.* 2002). Even the use of an adaptive threshold leads to limited results since it produces numerous look-alikes and small noisy blobs and demands and also requires extensive computational time (Gasull *et al.* 2002, Solberg *et al.* 1999, 2007).

In this paper, the detection of possible oil spills is performed by a geometric level set segmentation that acts globally in an image, in contrast to the pixel-based threshold or edge detection methods. These models are based on the theory of curve evolution and geometric flows and, in particular, on the mean curvature motion of Osher and Sethian (1998), with numerous successful applications for computer vision feature extraction tasks (Osher and Paragios 2003, Paragios *et al.* 2005) such as in medical image processing for detecting and tracking tumours, in industry for detection tasks during robot controlling processes, in modelling objects or environments, for visual surveillance, etc.

Global methods, aiming to understand how images can be segmented into meaningful regions, are one of the main problems of natural and computational vision (Tsai *et al.* 2001, Paragios *et al.* 2005). Let $I(x)$ (where x is a bi-variable (x, y)) be an image defined on a domain W without any particular geometrical structure. One of the key features is the segmentation process partitioning W into domains W_i, on which the image I is homogeneous and which are delimited by a system of crisp and regular boundaries (qualitative discontinuities) K.

In Bayesian models, two parts exist: the prior model and the data model. Here, the prior model takes *a priori* the phenomenological evidence of what is qualitatively a segmentation, namely an approximation of image I by piecewise smooth functions u on $W-K$, which are discontinuous along a set of edges K. The aim is to introduce a way of selecting, from among all the allowed approximations (u, K) of I, the best possible one.

For this, Mumford and Shah (1989) used an energy functional $E(u, K)$ that contains three terms:

1. A term that measures the variation and controls the smoothness of u on the open connected components W_i of $W-K$,
2. A term that controls the quality of the approximation of I by u and
3. A term that controls the length, the smoothness, the parsimony and the location of the boundaries K, and inhibits the spurious phenomenon of over-segmentation.

The Mumford and Shah (MS) energy that was implemented here, following the ideas of Chan and Vese (1999) and Tsai *et al.* (2001), is described by the following functional:

$$E(u, K) = \int_{W-K} |\nabla u|^2 \mathrm{d}x + \lambda \int_{W} (u-I)^2 + \mu \int_{K} \mathrm{d}\sigma. \quad (1)$$

Due to the coefficients λ and μ, the MS model is a multi-scale one: if μ is small, the output is a 'fine grained' segmentation, if μ is large, the output is a 'coarse grained' segmentation. As some regularity properties of boundaries can be deduced from the minimizing of E, the third term of the MS model is given in a more general setting (not *a priori* regular) by $H^1(K) = \int_K \mathrm{d}H^1$, where H^1 is the length of K in the Hausdorff sense (Mumford and Shah 1989), defined by $H^1(K) = \sup_{\varepsilon \to 0^+} H^1_\varepsilon(K)$, with:

$$H^1(K) = \inf \left\{ \sum_{i=1}^{i=\infty} \mathrm{diam} B_i : K \subseteq \bigcup_{i=1}^{i=\infty}, \mathrm{diam} B_i < \varepsilon \right\}. \quad (2)$$

K is covered in the less redundant way by small disks B_i and is approximated by the diameters of the B_i taking the limit for vanishing diameters. The above described energy functional (equation (1)) was implemented towards the segmentation of the sea surface on SAR imagery.

3. Developed methodology

A three-step methodology has been developed here, although a fourth one should also be implemented in cases where meteorological and oceanic data are available for a post-processing procedure (Girard-Ardhuin *et al.* 2003, Migliaccio *et al.* 2005). The structure of the developed SAR image processing methodology is presented in figure 1.

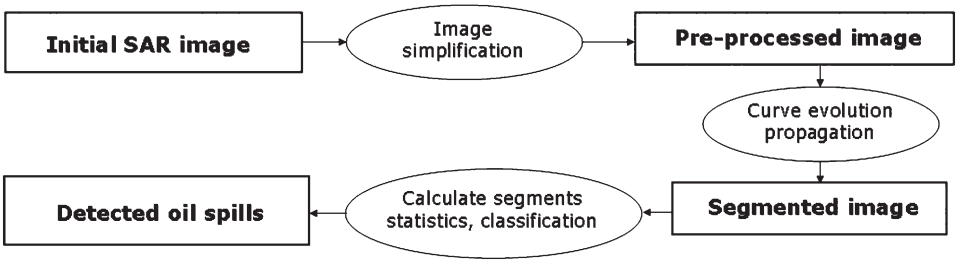

Figure 1. Structure of the developed SAR image processing methodology for automatic oil spill detection.

At first, a pre-processing step of image simplification has taken place. The applied pre-processing algorithm (Karantzalos and Argialas 2006, Karantzalos *et al.* 2007) consists of a combination of anisotropic diffusion filtering (ADF) and morphological levellings (ML). ADF and ML are nonlinear multi-scale operators with many interesting properties (Weickert 1998, Meyer and Maragos 2000, Soille and Pesaresi 2002). They can decrease initial image heterogeneity and highlight the distinction between image objects, so that, on the one hand, visual quality is improved and, on the other hand, edge detection and segmentation techniques also benefit. Especially with the use of ML filtering, details vanish from one scale to the next, while the contours of the remaining objects are preserved sharp and perfectly localized (Meyer and Maragos 2000). Hence, objects are enhanced so that the segmentation operator can detect where object boundaries are, avoiding time consuming processes in different images resolutions. In figure 2 (second row), the resulting enhanced, smoothed and simplified versions of the initial SAR image subscenes are shown. Several flat image intensity zones have been created and others have been extended towards facilitating image segmentation.

In the second step, the pre-processed image, which was a simplified version of the original, was segmented for the detection of all suspicious oil slicks while simultaneously preserving their shapes. Slicks appear with various shape deformations in SAR images (Brekke and Solberg 2005, figure 2, first row). Sea surface also appears complex in SAR images, as it is a combination of various intensities

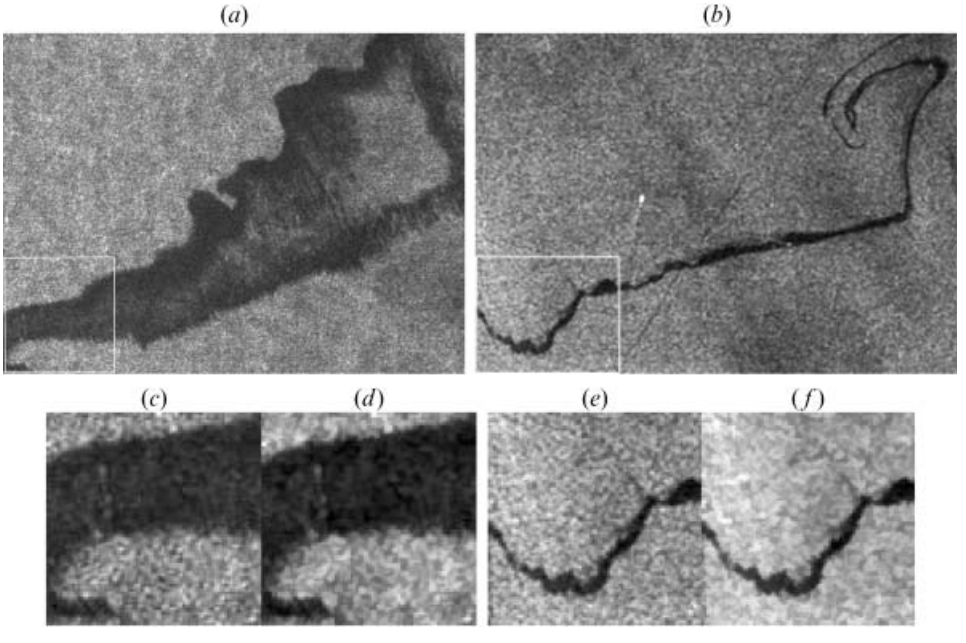

Figure 2. First row: oil spills appear with various shapes such as in (*a*) a subscene (approximately 500 × 400 pixels) of an ENVISAT advanced synthetic aperture radar (ASAR) wide swath mode (WSM) image acquired on 17 November 2002 (Galicia, Spain) ©ESA and (*b*) a subscene (approximately 300 × 200 pixels) of an ENVISAT ASAR WSM image acquired on 9 May 2005 (Gotland Island, Sweden) ©ESA. Second row: results from the algorithm's image simplification step. (*c*) and (*e*) are crops (marked in white on the first row) of the initial image. The resulting filtered images are (*d*) and (*f*), respectively.

representing certain atmospheric and oceanic phenomena and as the radar backscatter from the sea depends strongly on the incidence angle. To deal with this complexity, the previously described MS curve evolution algorithm was employed and implemented in a similar manner using the energy functionals that have been proposed by Chan and Vese (1999) and Tsai *et al.* (2001). The λ and μ level set coefficients from equation (1), were set equal to one. However, they can be tuned to optimize oil spill detection in cases where the wind level (i) is *a priori* known, (ii) is inspected in the image visually or (iii) is estimated from the SAR image by applying an inverted CMOD4 model (Salvatori *et al.* 2003).

The last step in the developed processing scheme is the classification of pure oil spills and look-alikes. The following statistical measurements (regional descriptors) were calculated for each of the detected segments: area, perimeter, shape complexity, eccentricity, orientation, segments mean border gradient, inside segments standard deviation and outside segments area standard deviation. Depending on the above mainly geometric and shape characteristics, the final detected oil spills were extracted, along with a suggestive assignment of the decision's confidence levels, with the use of a minimum distance classifier. More feature extraction metrics, such as, for example, those that describe the texture in and around segments, and the use of an advanced classifier may yield better results. In this study, though, the interest was, mainly, to improve the quality of the classification's input, as it plays a key role in the overall detection result. In all cases, manual verification will be an essential step, after the activation of an alarm, indicating a high probability of the existence of an oil spill.

4. Experimental results and discussion

The developed scheme has been applied to and tested on about fifteen ERS and ENVISAT SAR images, which are available from the ESA Earthnet Online catalogue (http://earth.esa.int/ew/oil_slicks/) and the CEARAC SAR image database (CEARAC database 2003). Since a standard evaluation dataset, with known ground truth (the oil spill has been verified by an operational aircraft), were not available, a quantitative comparison with the results of other methodologies (Solberg *et al*. 1999, 2007, Del Frate *et al.* 2000, Fiscella *et al.* 2000) could not be performed. The evaluation of the developed methodology was based on the photo-interpretation carried out by a human operator. Moreover, the above research efforts have been performed on different datasets and thus a direct quantitative comparison cannot be achieved. Knowledge or predictions of wind measurements were not available, thus making a fine tuning of the λ and μ level set coefficients and the calculation of relevant regional descriptors impossible. The developed methodology included a sensor specific set of parameters due to the different spatial resolution, intensity variations and the contrast of ERS and ENVISAT sensors. However, the ENVISAT ASAR WSM images acquired at VV-polarization were, in general, preferred due to their wide swath and greater contrast between oil spill and surrounding water (Alpers and Espedal 2004).

In the following two subsections, the level set segmentation, with and without a pre-processing step, is compared to threshold-based and edge detection techniques. Moreover, experimental results from its application for the detection of different oil spill shapes are also presented. The developed algorithm's efficiency, for real-time detection and tracking of oil spills, is also demonstrated and discussed in §4.3.

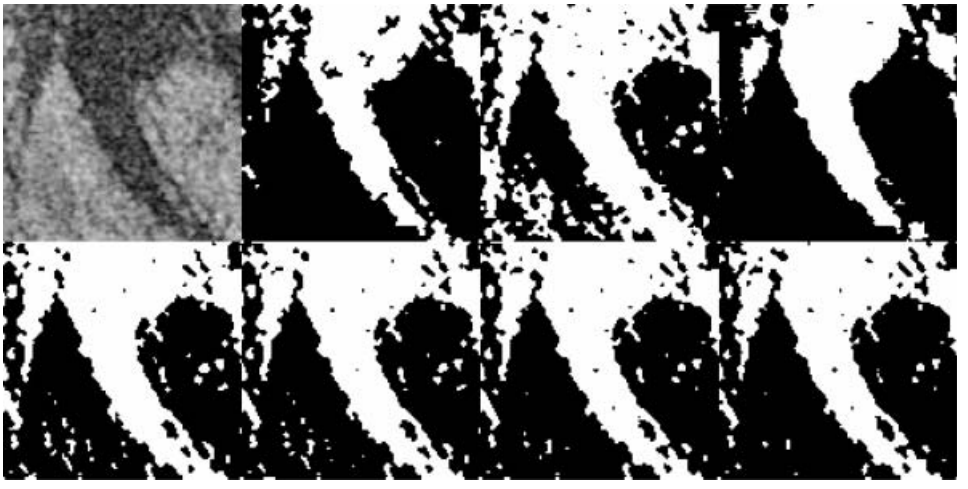

Figure 3. Different types of segmentation for the detection of possible oil slicks. First row: a subscene of an ENVISAT ASAR WSM image (first image from left) acquired on 29 August 2006 (Guimaras, Philippines) ©ESA. Binary result after the application of the hysteresis threshold (second image), the adaptive threshold (third image) and the level set technique (last image). Second row: binary results after the application of a constant threshold with a value equal to the image's mean value (first image from the left), 2.5% lower than the image's mean value (second image), 5% lower than the image's mean value (third image) and 7.5% lower than the image's mean value (last image).

4.1 *Comparing the level set segmentation with threshold-based and edge detection techniques*

Three threshold-based and edge detection techniques were compared with the level set segmentation for the detection of possible oil spills. In figure 3, an adaptive, a hysteresis and four constant threshold values are applied to a subscene (approximately 30 000 pixels) of an ENVISAT ASAR WSM image and their segmentation binary results are presented and compared with the output of the level set segmentation. For a quantitative evaluation, the number of the resulting segments of each method is presented in table 1. The level set segmentation leads to the minimum number of output segments (22 segments were detected, whereas in the threshold-based methods, there were 31 to 48). Binary results indicate that, although all methods did detect dark areas in the image, the threshold-based method leads to an over-segmentation output, due to their pixel-based nature. Furthermore, as it can

Table 1. Quantitative measures indicating the number of output segments (possible oil spills) produced by different methods. Level set segmentation leads to the minimum number of segments.

Method	Adaptive threshold	Hysteresis threshold	Level set	Edge detection
Number of segments	37	31	22	46
Method	Threshold (mean value)	Threshold (2.5% lower than mean)	Threshold (5% lower than mean)	Threshold (7.5% lower than mean)
Number of segments	48	46	37	35

be observed in figure 3, with the threshold-based techniques, the main body of the possible oil spill was detected containing a significant number of holes and gaps. In contrast, the level set segmentation managed to extract successfully the whole body of the oil spill.

The above qualitative comparison can also be supported by observations made in figure 4, where the resulting segment boundaries shown in green were overlaid on the initial image (first row) and the output segments were labelled and pictured with a different colour in the second row. Given that region descriptors (i.e. the input to classification) are being computed on these output segments, the importance of a compact segmentation output is clear. Descriptors that are based on compact and geometrically accurately defined objects can efficiently describe their shape, geometry and texture and thus improve the subsequent classification procedure. In the third row of figure 4, the result from the application of the Canny edge detector (Canny 1986) is presented. The edge detector managed to extract all abrupt changes in image intensities, as is shown when edges (in red) are overlaid on the initial image (third row, middle). Forty-six edges were extracted and have to be

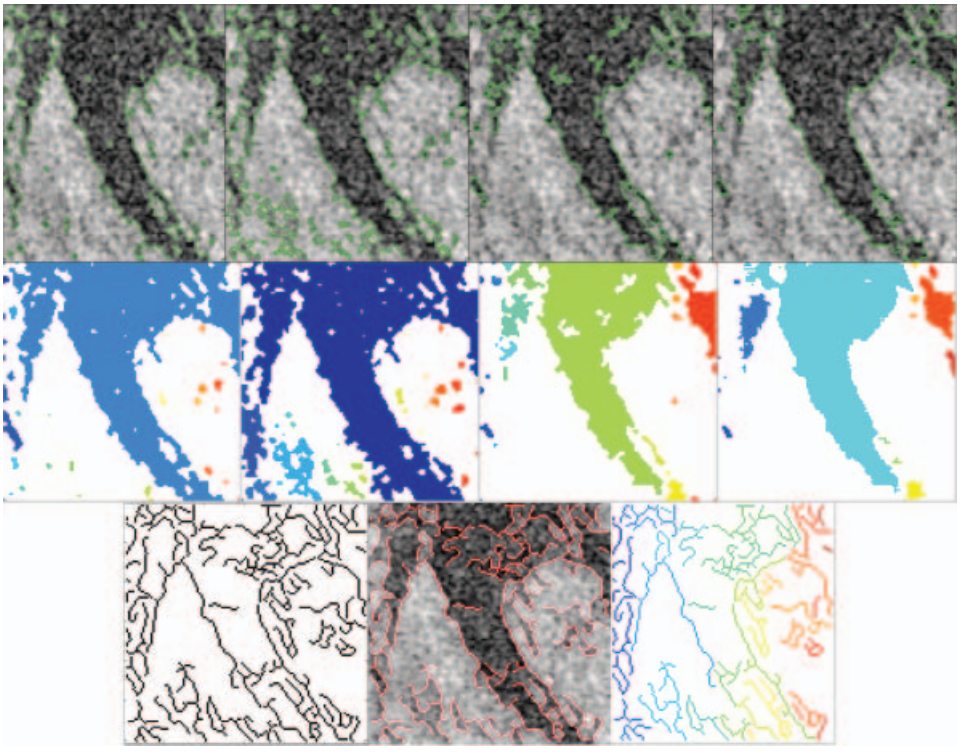

Figure 4. Comparing different types of segmentation for the detection of possible oil slicks in the ENVISAT image of figure 3. First row: resulting segment boundaries (green) overlaid on the initial image after the application of a constant threshold of 7.5% lower than the image's mean value (first image from the left), an adaptive threshold (second image), a hysteresis threshold (third image) and the level set segmentation. Second row: labelled segments/objects. Each labelled segment is presented with a different colour. The number of segments extracted can be found in table 1, and columns are corresponding to the methods used in the previous row. Third row: binary image after the application of the Canny edge detector to the initial image (first image), edges (in red), overlaid on the initial image (second image) and labelled edges, each one with a different colour (last image).

linked to form segments for further processing. Linking edges is not a trivial operation and demands certain procedures constraining output segments to form unique and closed objects. Such operations are computational intensive compared with the level set segmentation.

In figure 5, results from the application of two threshold-based methods and the level set segmentation are presented. Methods were applied to the two ENVISAT ASAR WSM images of figure 2, on which two different oil slicks with different shapes are shown. For the first case (first two rows), the detection procedure, according to a human expert's reasoning, should extract one segment that corresponds to the whole oil spill area (area with low intensity values). However, the threshold-based techniques produced a number of noisy dark blobs and also certain gaps and holes inside the main oil spill segment. These features will impede a classifier towards the discrimination of the look-alikes. It should be noted (table 2) that the level set technique resulted in only two output segments, whereas with the threshold-based techniques, 25 segments were extracted.

Furthermore, for the detection of a thin curvy linear oil spill, the two threshold-based methods lead to an over-segmentation result. In contrast, the level set technique detected only two segments, approaching human perception. Threshold-based techniques resulted in about 80 output segments (table 2) making the subsequent classification procedure much more complicated. In addition, for classifiers requiring training, such segments, which do not describe sea surface features well, increase the variation of the reported statistical descriptor values that are used for the discrimination with the look-alikes. Moreover, as can be seen from the output labelled segments (figure 5, last row) only the level set technique managed to detect the whole oil spill as one compact object/segment, in contrast to the threshold-based techniques where the oil spill was divided into two or three different parts.

4.2 *Applying level sets for the detection of possible oil spills*

In figure 6, the different steps of the level set curve propagation are demonstrated for the three oil spill cases presented in the above figures. Different steps correspond to iterations with which the solution of the energy functional (equation (1)) was approximated. Starting from an initial arbitrary elliptical curve, the level set propagates, ending up at the final segmentation output, where the possible oil spill boundaries have been detected. In all cases, the curve evolution energy functional managed to successfully extract possible oil spill boundaries, avoiding over-segmentation and describing the geometry and the shape of oil spills (and look-alikes) well; this was because output segments were compact, without gaps or holes. As can be observed by a close look, the evolving curve(s) propagate robustly, avoiding local minima and are stopped in the boundaries of homogeneous regions, approximating the result of a segmentation carried out by an operator. In addition, the evolving curve(s) cope well with abrupt shape deformations and splits.

Furthermore, oil spills were detected in real-time (approximately 8 s was the computation time for each image of figure 6 using a moderate Pentium-V computer). For the processing of the entire ENVISAT ASAR WSM image (with a coverage of 400×400 km and an image size of 5400×5400 pixels), the result from the level set segmentation was obtained approximately after 3 min of computing on a PC with 1 GB RAM. The source code of the algorithm was implemented in ©Matlab. Given prior experience in similar problems, an optimization of the code should reduce

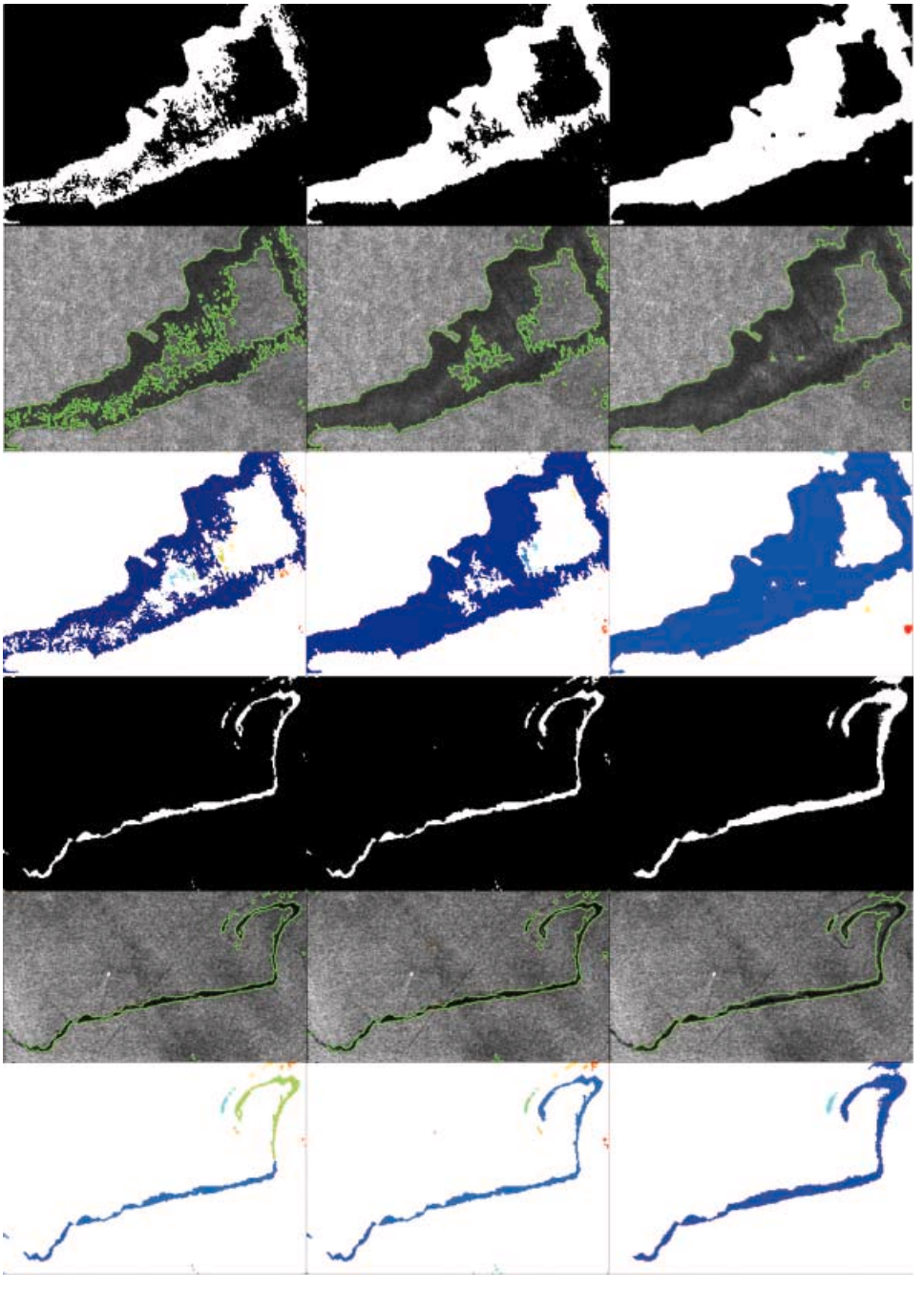

Figure 5. Results from the application of different segmentation techniques for the detection of possible oil slicks in the ENVISAT images of figure 2. First and fourth row: binary outputs after the application of a constant threshold 2.5% lower value than the image's mean (left), a hysteresis threshold (middle) and the level set technique (right). Second and fifth rows: previous results with the output segments boundaries overlaid (in green) on the initial image. Third and sixth rows: labelled segments/objects. Each labelled segment is presented with a different colour. The number of segments extracted can be found in table 2.

Table 2. Quantitative measures indicating the number of output segments (possible oil spills) produced by different applied methods for the two images of figure 2. Level set segmentation leads to the minimum number of segments.

		Methods		
	Initial image:	Constant threshold	Hysteresis threshold	Level sets
Number of detected segments	Figure 2(*a*)	25	25	2
	Figure 2(*b*)	90	85	4

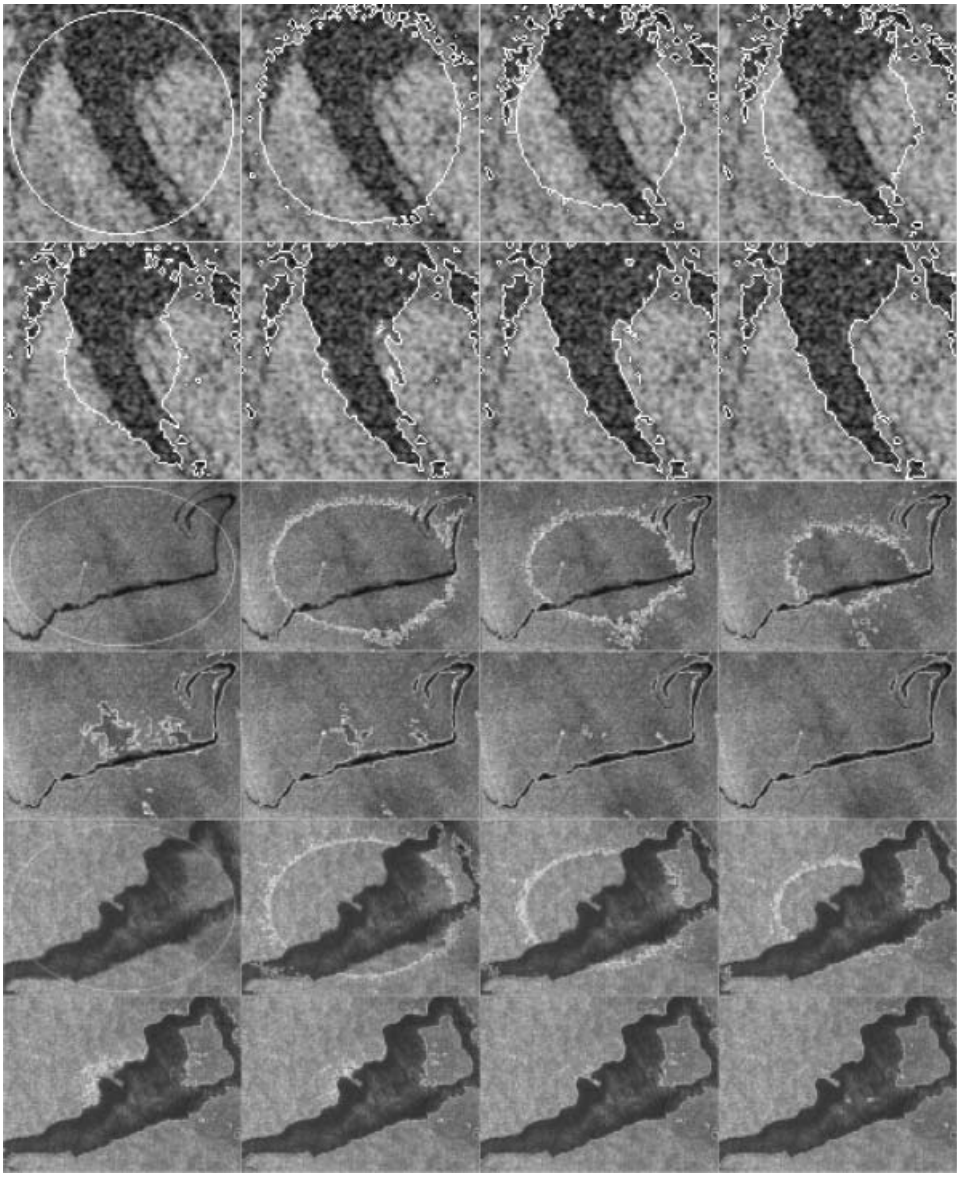

Figure 6. Applying the level set curve propagation algorithm to the three ENVISAT images shown in figures 3 and 5. The different steps of the curve evolution propagation are shown, starting from an initial arbitrary elliptical curve leading to the final possible oil spill detected boundaries. View this figure starting each row from the left.

computational time to less than 10 s. Such optimizations of the level set technique have already been proposed for other computer vision applications (Osher and Paragios 2003, Paragios *et al.* 2005). Videos demonstrating the curve propagation of the level set based segmentation can be viewed at the author's website http://www.mas.ecp.fr/vision/Personnel/karank/Demos/oil.

4.3 *Real-time detection and tracking of oil spills*

Adding up the computational time required for all the steps of the developed methodology it is estimated that a total of approximately 8 min is required for the processing of an entire ENVISAT ASAR WSM image. These 8 min can be reduced to less than 0.5 min by optimizing the source code. Moreover, the computational demanding step for region descriptor calculations of each detected segment (possible oil spill) can be optimized and computed in a parallel multi-grid framework, as the calculations of each segment attributes could be derived in parallel.

Level sets have been extensively used for the tracking of moving objects in numerous computer vision applications (Karantzalos and Paragios 2005, Paragios *et al.* 2005). In the same way, level sets were tested for the task of tracking oil spills in a temporal sequence of SAR images, providing that their geo-reference is known *a priori*. Note that the geo-reference of the initial image is also necessary for the application of a land mask to it and to avoid processing over land areas.

Real-time conditions were modelled, and the developed methodology was tested for the detection and tracking of oil spills. In figure 7, results from the application of the developed algorithm to a sequence of three ENVISAT ASAR WSM images are presented. These images, acquired on different days, are described with a significant variance in image intensity values, contrast and shape of shown objects. In the second row, the resulting binary images after the application of the first two steps of the developed algorithm are presented. Image simplification and segmentation resulted into about 80 (first column), 250 (second column) and 280 (last column) segments, respectively. The resulting possible oil spills detected by the classification procedure, are shown in the last two rows. Eight (first column), 53 (second column) and 50 (last column) oil spills were detected from the developed algorithm. After a close look in the figure, one can see that the algorithm did manage to successfully detect possible oil spills and preserve efficiently, in terms of spatial accuracy, their boundaries and shape. In cases where a tight temporal acquisition sequence is available, the detected oil spills from the first frame can be used to form the initial curve for the level set propagation in the second one. Thus, the tracking of the spills could become much faster and reduce the computational time by half.

5. Conclusions and future perspectives

In this paper, a SAR image processing scheme for the real-time detection and tracking of oil spills was developed. The developed methodology consists of a pre-processing step, in which an advanced image simplification, followed by a geometric level set segmentation for the detection of possible oil spills take place. Finally, a classification was performed for the separation of look-alikes, leading to oil spill extraction. Experimental results demonstrate that the level set segmentation is a robust tool for the detection of possible oil spills, copes well with abrupt shape deformations and splits and outperforms earlier efforts that were based on different types of thresholds or edge detection techniques. The level set segmentation

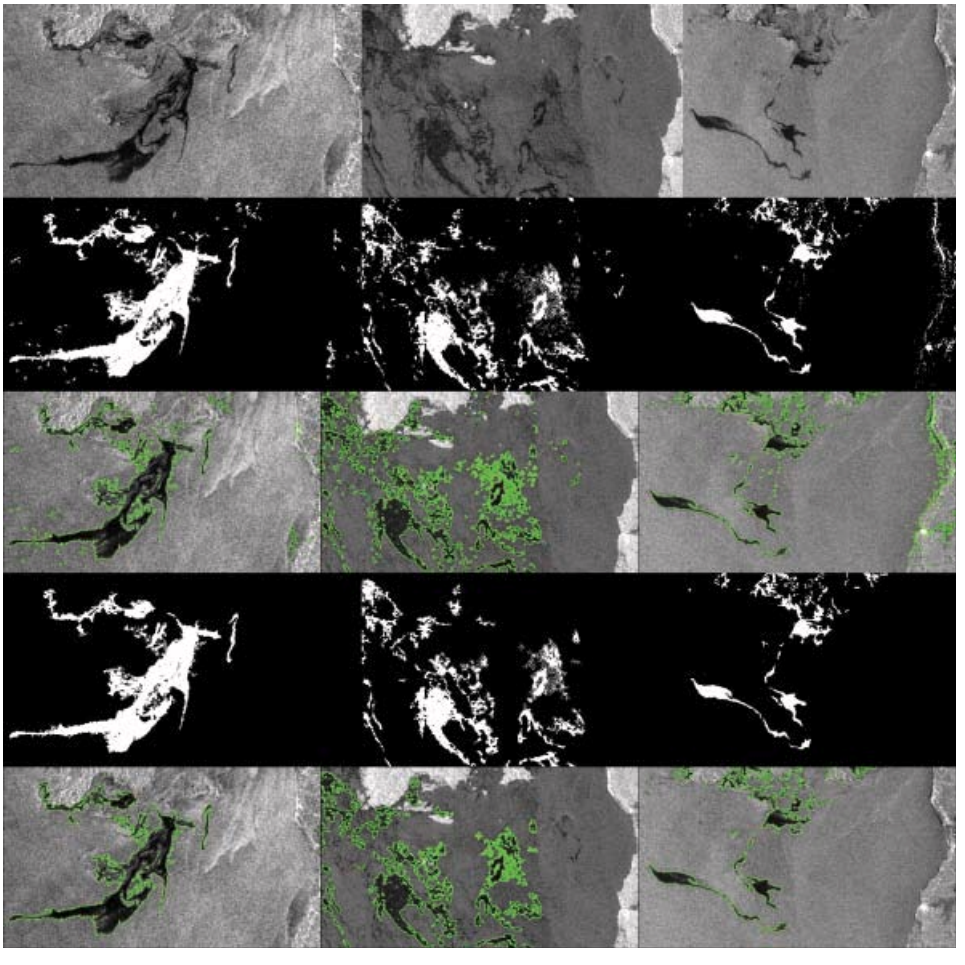

Figure 7. Applying the developed algorithm to a sequence of ENVISAT images acquired on 24, 28 and 29 August 2006 (Guimaras, Philippines) ©ESA. First row: initial images. Second row: resulting binary images after the application of the first two steps of the developed algorithm. Third row: resulting segments boundaries overlaid (in green) on the initial image. Fourth row: detected oil slicks after the classification procedure. Last row: detected oil slicks overlaid (in green) on the initial image.

produced a compact result without holes or gaps segments, avoided over-segmentation and resulted into a sufficient spatial precision regarding the boundaries of output segments.

A quantitative comparison with the results of other methodologies (Del Frate *et al.* 2000, Solberg *et al.* 1999, 2007, Fiscella *et al.* 2000) could not be performed as we did not have access to data with available ground truth (the oil spill has been verified by an operational aircraft). Such an evaluation is anticipated. There is a need for a freely available dataset, containing more than 100 images per sensor, in which oil spills have been verified by a surveillance aircraft, in order for the research and development community to carry out algorithm testing in a constant framework. Our interest here has focused mainly on the optimization of the two first steps of the developed processing scheme, and the use of a more advanced classifier and more region descriptors is a subject for further research. In this

direction, a combination of a support vector machine classifier with an expert system decision support system is currently under implementation. Last but not least, for the construction of a SAR image processing operational system, optimization of the source code is necessary, along with an extensive evaluation of its results and fine tuning of all its parameters. Knowledge, or predictions, of the wind level and other meteorological and oceanic data will be of great importance during the main and the post-processing procedures.

Acknowledgements
We would like to thank the reviewers for their attentive review and constructive comments and suggestions.

References

Al-Khudhairy, D., 2002, *Marine Oil Pollution: Technologies and Methodologies for Detection and Early warning*. Technical Report, EC, Joint Research Centre.

Alpers, W. and Espedal, H., 2004, *Oils and Surfactants, Synthetic Aperture Radar Marine User's Manual*, C.R. Jackson and J.R. Apel (Eds), 11, pp. 263–275, National Oceanic and Atmospheric Administration (NOAA).

Argialas, D. and Harlow, C., 1990, Computational image interpretation models: an overview and a perspective. *Photogrammetric Engineering and Remote Sensing*, **56**, pp. 871–886.

Barni, M., Betti, M. and Mecocci, A., 1995, A fuzzy approach to oil spill detection on SAR images. In *International Geoscience and Remote Sensing Symposium*, **1**, pp. 157–159.

Bern, T.I., Wahl, T., Anderssen, T. and Olsen, R., 1992, Oil spill detection using satellite based SAR: experience from a field experiment. In *Proceedings of 1st ERS-1 Symposium*, Cannes, France, pp. 829–834.

Brekke, C. and Solberg, A.H.S., 2005, Oil spill detection by satellite remote sensing. *Remote Sensing of Environment*, **95**, pp. 1–13.

Canny, J., 1986, A computational approach to edge detection. *IEEE Transactions of Pattern Analysis and Machine Intelligence*, **8**, pp. 679–714.

CEARAC database of satellite SAR images, 2003, ©ESA. Available online at: http://cearac.poi.dvo.ru/en/db/ (accessed July 2006).

Chan, T. and Vese, L., 1999, An active contour model without edges. In *Proceedings of 2nd International Conference on Scale-Space*, Greece, pp. 141–151.

Change, L.Y., Chen, K.S., Chen, C.F. and Chen, A.J., 1996, A multiplayer-multiresolution approach to detection of oil slicks using ERS SAR image. In *Proceedings of 17th Asian Conference of Remote Sensing*, Sri Lanka.

Chen, C.F., Chen, K.S., Chang, L.Y. and Chen, A.J., 1997, The use of satellite imagery for monitoring coastal environment in Taiwan. In *International Geoscience and Remote Sensing Symposium*, **3**, pp. 1424–1426.

Del Frate, F., Petrocchi, A., Lichtenegger, J. and Calabresi, G., 2000, Neural networks for oil spill detection using ERS-SAR data. *IEEE Transactions on Geoscience and Remote Sensing*, **38**, pp. 2282–2287.

European Maritime Safety Agency (EMSA), 2007, EMSAs view on the GMES programme of EU and ESA, Lisbon, 4 June 2007. Available online at: http://cleanseanet.emsa.europa.eu/docs/public/index.html.

Espedal, H.A. and Johannessen, O.M., 2000, Detection of oil spills near offshore installations using synthetic aperture radar (SAR). *International Journal of Remote Sensing*, **21**, pp. 2141–2144.

Fingas, M.F. and Brown, C.E., 1997, Review of oil spill remote sensing. *Spill Science and Technology Bulletin*, **4**, pp. 199–208.

FISCELLA, B., GIANCASPRO, A., NIRCHIO, F., PAVESE, P. and TRIVERO, P., 2000, Oil spill detection using marine SAR images. *International Journal of Remote Sensing*, **21**, pp. 3561–3566.

GASULL, A., FABREGAS, X., JIMENEZ, J., MARQUES, F., MORENO, V. and HERRERO, M.A., 2002, Oil spills detection in SAR images using mathematical morphology. In *European Signal Processing Conference*, Toulouse, France, **1**, pp. 25–28.

GIRARD-ARDHUIN, F., MERCIER, G. and GARELLO, R., 2003, Oil slick detection by SAR imagery: potential and limitation. In *Proceedings of OCEANS 2003*, **1**, pp. 164–169.

INDREGARD, M., SOLBERG, A. and CLAYTON, P., 2004, *D2 – Report on Benchmarking Oil Spill Recognition Approaches and Best Practice*, Oceanides project, European Commission, archive no. 04-10225-A-Doc, contract no. EVK2-CT-2003-00177, technical report. Available online at: http://oceanides.jrc.cec.eu.int.

JENSEN, J.R., 2000, *Remote Sensing of the Environment: an Earth Resource Perspective* (Saddle River, NJ: Prentice Hall).

KANAA, T.F.N., TONYE, E., MERCIER, G., ONANA, V.P., NGONO, J.M., FRISON, P.L., RUDANT, J.P. and GARELLO, R., 2003, Detection of oil slick signatures in SAR images by fusion of hysteresis thresholding responses. In *International Geoscience and Remote Sensing Symposium*, **4**, pp. 2750–2752.

KARANTZALOS, K. and ARGIALAS, D., 2006, Improving edge detection and watershed segmentation with anisotropic diffusion and morphological levelings. *International Journal of Remote Sensing*, **27**, pp. 5427–5434.

KARANTZALOS, K. and PARAGIOS, N., 2005, Implicit free-form-deformations for multi-frame segmentation and tracking. In *IEEE Variational and Level Set Methods in Computer Vision*, Lecture Notes in Computer Science, Springer, **3752**, pp. 271–282.

KARANTZALOS, K., ARGIALAS, D. and PARAGIOS, N., 2007, Comparing morphological levelings constrained by different markers. *ISMM*, G.J.F. Banon, J. Barrera, and U.M. Braga-Neto (Eds). *Mathematical Morphology and its Applications to Signal and Image Processing*, pp. 113–124.

KERAMITSOGLOU, I., CARTALIS, C. and KIRANOUDIS, C.T., 2006, Automatic identification of oil spills on satellite images. *Environmental Modelling and Software*, **21**, pp. 640–652.

LILLESAND, T., KIEFER, R. and CHIPMAN, J., 2003, *Remote Sensing and Image Interpretation*, 5th edn (New York: John Wiley & Sons).

LIU, A.K., PENG, C.Y. and CHANG, S.Y.-S., 1997, Wavelet analysis of satellite images for costal watch. *IEEE Journal of Oceanic Engineering*, **22**, pp. 9–17.

MEYER, F. and MARAGOS, P., 2000, Nonlinear scale–space representation with morphological levelings. *Journal of Visual Communication and Image Representation*, **11**, pp. 245–265.

MIGLIACCIO, M., TRANFAGLIA, M. and ERMAKOV, A., 2005, A physical approach for the observation of oil spills in SAR images. *IEEE Journal of Oceanic Engineering*, **30**, pp. 496–507.

MUMFORD, D. and SHAH, J., 1989, Optimal approximation by piecewise smooth functions and associated variational problems. *Communications on Pure and Applied Mathematics*, **42**, pp. 577–685.

OSHER, S. and PARAGIOS, N., 2003, *Geometric Level Set Methods in Imaging Vision and Graphics* (Berlin: Springer Verlag).

OSHER, S. and SETHIAN, J., 1988, Fronts propagation with curvature dependent speed: algorithms based on Hamilton–Jacobi formulations. *Journal of Computation Physics*, **79**, pp. 12–49.

PARAGIOS, N., CHEN, Y. and FAUGERAS, O., 2005, *Handbook of Mathematical Models in Computer Vision* (Berlin: Springer).

PERONA, P. and MALIK, J., 1990, Scale space and edge detection using anisotropic diffusion. *IEEE Pattern Analysis Machine Intelligence*, **12**, pp. 16–27.

SALVATORI, L., BOUCHAIB, S., FRATE, F.D., LICHTENNEGER, J. and SAMARA, Y., 2003, Estimating the wind vector from radar SAR images when applied to the detection of

oil spill pollution. In *International Symposium on GIS and Computer Cartography for Coastal Zone Management*. Available online at: www.gisig.it/coastgis/programma/abstract_poster/smara.htm.

SKØELV, A. and WAHL, T., 1993, *Oil Spill Detection Using Satellite Based SAR*, Phase 1B competition report. Technical report, Norwegian Defence Research Establishment.

SOILLE, P. and PESARESI, M., 2002, Advances in mathematical morphology applied to geoscience and remote sensing. *IEEE Transactions on Geosciences and Remote Sensing*, **40**, pp. 2042–2055.

SOLBERG, A.H.S., DOKKEN, S.T. and SOLBERG, R., 2003, Automatic detection of oil spills in Envisat, Radarsat and ERS SAR images. In *Geoscience and Remote Sensing Symposium*, **4**, pp. 2747–2749.

SOLBERG, A.H.S., BREKKE, C. and HUSØY, P.O., 2007, Oil spill detection in RADARSAT and ENVISAT SAR images. *IEEE Transactions on Geosciences and Remote Sensing*, **45**, pp. 746–755.

SOLBERG, A.H.S., STORVIK, G., SOLBERG, R. and VOLDEN, E., 1999, Automatic detection of oil spills in ERS SAR images. *IEEE Transactions on Geoscience and Remote Sensing*, **37**, pp. 1916–1924.

TSAI, A., YEZZI, A. and WILLSKY, A., 2001, Curve evolution implementation of the Mumford–Shah functional for image segmentation, denoising, interpolation, and magnification. *IEEE Transactions on Image Processing*, **10**, pp. 1169–1186.

WAHL, T., SKOELV, A. and ANDERSEN, J.H.S., 1994, Practical use of ERS-1 SAR images in pollution monitoring. *International Geoscience and Remote Sensing Symposium*, **4**, pp. 1954–1956.

WEICKERT, J., 1998, *Anisotropic Diffusion in Image Processing* (Stuttgart: Teubner).

WU, S.Y. and LIU, A.K., 2003, Towards an automated ocean feature detection, extraction and classification scheme for SAR imagery. *International Journal of Remote Sensing*, **24**, pp. 935–951.